MATHEMATICAL AND PHYSICAL MODELING OF FLOW-INDUCED VIBRATIONS OF HUMAN VOCAL FOLDS

Petr Šidlof
Institute of Thermomechanics, Academy of Sciences of the Czech Republic, Prague, Czech Republic and Faculty of Mechatronics, Technical University of Liberec, Czech Republic

Olivier Doaré & Olivier Cadot & Antoine Chaigne
École Nationale Supérieure de Techniques Avancées, Paris, France

Jaromír Horáček
Institute of Thermomechanics, Academy of Sciences of the Czech Republic, Prague, Czech Republic

ABSTRACT

The pressure and velocity fields in coronal plane along the vibrating vocal folds were studied using a finite element mathematical model. The shapes of the vocal folds were specified according to data measured on excised human larynges in phonation position. The mathematical model of the flow is based on 2D incompressible Navier-Stokes equations adapted to deal with the time-variable shape of the domain, caused by vocal fold vibration. The numerical simulations allow to observe closely various flow features related to phonation - flow separation in the glottis, Coanda effect or vortex shedding.

The numerical results were verified experimentally by Particle Image Velocimetry (PIV) on a physical vocal fold model. In addition to acoustic, subglottal pressure and impact intensity measurements, flow velocity fields were recorded in the domain immediately above glottis. Analysis of the PIV images taken within 25 phases of one vibration cycle gives good insight into the dynamics of the supraglottal flow.

1. INTRODUCTION

Human voice is created by passage of the airflow between vocal folds, which are located in the upper part of larynx. The vocal folds (formerly called vocal cords) are two symmetric soft tissue structures fixed between the thyroid cartilage and arytenoid cartilages (which are paired); basically they are composed of the thyroarytenoid (TA) muscle and ligament covered by mucosa.

When air is expired from lungs, the constriction formed by the vocal folds (which is called *glottis*) induces acceleration of the flow; under certain circumstances (subglottal pressure, glottal width, longitudinal tension in the TA and ligament) the fluid-structure interaction may invoke vocal fold oscillations. It is important that the vibration is a passive process – when voicing, people do not perform any sort of periodic muscle contraction, they only adjust the initial configuration and let the vocal folds vibrate by the airflow.

The flow is modeled by incompressible nonstationary Navier-Stokes equations in 2D, solved by the finite element method (FEM). The Navier-Stokes equations were first reformulated in arbitrary Lagrangian-Eulerian (ALE) approach. The Navier-Stokes equations are nonlinear; this is why it was necessary to use a suitable linearization of the convective term. The geometry of the problem, i.e. the 2D shape of the vocal folds and adjoining vocal tract, was specified according to measurements on excised human larynges, performed in the Institute of Thermomechanics (Šidlof et al, 2004).

The results from the mathematical models should always be verified using experimental data. Since the human vocal folds are hardly accessible, the majority of processes occurring during phonation cannot be measured directly in vivo. This is why many physical vocal fold models with well-defined and easily controllable parameters have been developed in recent years – like the self-oscillating latex-tube model of Deverge et al (2003), the driven scaled models of Kob et al (2005); Erath et al (2006) or the self-oscillating 1:1 vocal fold model of Thomson et al (2005).

Investigation of the supraglottal flow velocity field represents one of the cases, where both in vivo and in vitro measurements are hardly realizable. Therefore a self-vibrating mechanical model of human vocal folds was designed and fabricated at ENSTA Paris. The principal goal was

to study the conditions, where flow-induced vibrations of vocal folds occur and to investigate the velocity fields in the supraglottal channel immediately upstream the narrowest glottal gap by means of Particle Image Velocimetry (PIV).

2. MATHEMATICAL MODEL

Let $\Omega_t \subset \mathbb{R}^2$ be the (time-variable) domain occupied by the fluid. The boundary $\Gamma = \partial\Omega$ is composed of four non-intersecting parts (see Fig. 1): $\Gamma = \Gamma_{in} \cup \Gamma_{out} \cup \Gamma_{wall} \cup \Gamma_{VF}$, where Γ_{in} and Γ_{out} are virtual boundaries representing the inlet and outlet, $\Gamma_{wall} = \Gamma^{b1}_{wall} \cup \Gamma^{b2}_{wall} \cup \Gamma^{u1}_{wall} \cup \Gamma^{u2}_{wall}$ is the fixed wall, which is not a function of time, and $\Gamma_{VF} = \Gamma^{b}_{VF} \cup \Gamma^{u}_{VF}$ stands for the surface of the moving vocal folds. The superscripts 'b' and 'u' denote the bottom and upper parts, respectively.

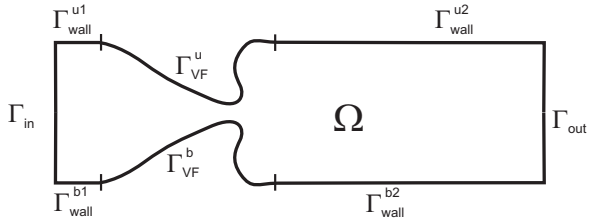

Figure 1: Sketch of the computational domain and definition of its boundary parts.

Our goal is to find the flow velocity $\boldsymbol{u}(t, \boldsymbol{x})$, kinematic pressure $p(t, \boldsymbol{x})$ and generalized coordinates of the bottom and upper vocal folds $q^b_i(t)$, $q^u_j(t)$, $t \in (0, T)$, $x \in \Omega_t$.

Since the Eulerian time derivative $\partial/\partial t$ is not well defined in a time-dependent computational domain Ω_t, the standard, Eulerian form of the Navier-Stokes equations is not suitable for description of the flow in a domain that deforms in time. Therefore it will be reformulated using arbitrary Lagrangian-Eulerian approach.

The ALE-formulation of the Navier-Stokes equations reads

$$\frac{D^A}{Dt}\,\boldsymbol{u} + \Big[(\boldsymbol{u} - \boldsymbol{w}) \cdot \nabla\Big]\boldsymbol{u} + \nabla p - \nu\,\Delta\boldsymbol{u} = 0$$
$$\operatorname{div} \boldsymbol{u} = 0 \quad , \tag{1}$$

where $\boldsymbol{w}$ is the *domain velocity* (velocity of the meshpoints) and $\frac{D^A}{Dt}$ is so-called *ALE-derivative*, which can be easily discretized even in time-dependent computational domains.

Setting the boundary conditions represents a rather delicate question. On the outlet Γ_{out}, one possible choice is the "do-nothing condition" (Turek, 1999)

$$-\nu\frac{\partial \boldsymbol{u}}{\partial \boldsymbol{n}}(t, \boldsymbol{x}) + p(t, \boldsymbol{x})\,\boldsymbol{n}(\boldsymbol{x}) = p_{ref}\,\boldsymbol{n}(\boldsymbol{x})$$
$$\text{for } \boldsymbol{x} \in \Gamma_{out},\ t \in [0, T]\ , \tag{2}$$

where $\partial/\partial\boldsymbol{n}$ denotes the normal derivative, $\boldsymbol{n}(\boldsymbol{x})$ is the unit outer normal to Γ_{out} and p_{ref} is the reference pressure. In certain cases, however, this condition becomes too vague – it does not even prevent the flow returning to the domain Ω through Γ_{out}. Thus, the total influx into the domain Ω can grow infinite and the numerical scheme tends to diverge. To suppress this inconvenience, the boundary condition (2) can be slightly modified during the derivation of the weak formulation of the equations.

On the inlet Γ_{in}, two conditions were tested: either a parabolic profile of the vertical velocity component, or the (modified) do-nothing condition as on Γ_{out}. The difference $p^{in}_{ref} - p^{out}_{ref}$ then represents the transglottal pressure (approximately equal to the lung pressure during phonation), which drives the flow.

Since we use a viscous model, the "no-slip condition" is prescribed on the fixed walls Γ_{wall}. On the moving vocal fold surfaces, the velocity of the fluid particles must be equal to the velocity of the moving surface, which is given by the domain velocity $\boldsymbol{w}$.

For the numerical solution of the Navier-Stokes equations (1), these need first to be semidiscretized in time. A constant timestep τ was used. Let us define the discrete time level $t_i = i\,\tau$ and the approximate flow velocity, pressure and domain velocity on this time level $\boldsymbol{u}^i(\boldsymbol{x}) \approx \boldsymbol{u}(t_i, \boldsymbol{x})$, $p^i(x) \approx p(t_i, \boldsymbol{x})$ $\boldsymbol{w}^i(x) \approx \boldsymbol{w}(t_i, \boldsymbol{x})$, $\boldsymbol{x} \in \Omega_{t_i}$. If we denote the ALE-maps of the reference point $\boldsymbol{X}$ on the three time levels involved $\boldsymbol{x}^{n+1} = A_{t_{n+1}}(\boldsymbol{X})$, $\boldsymbol{x}^n = A_{t_n}(\boldsymbol{X})$, $\boldsymbol{x}^{n-1} = A_{t_{n-1}}(\boldsymbol{X})$, the ALE-derivative can be approximated by the formula

$$\frac{D^A\boldsymbol{u}}{Dt}(t_{n+1}, \boldsymbol{x}_{n+1}) \approx$$
$$= \frac{3\,\boldsymbol{u}^{n+1}(\boldsymbol{x}_{n+1}) - 4\,\boldsymbol{u}^n\big(A_{t_n}\big(A^{-1}_{t_{n+1}}(\boldsymbol{x}_{n+1})\big)\big)}{2\,\tau} +$$
$$\frac{\boldsymbol{u}^{n-1}\big(A_{t_{n-1}}\big(A^{-1}_{t_{n+1}}(\boldsymbol{x}_{n+1})\big)\big)}{2\,\tau}\ . \tag{3}$$

Provided that the ALE-mappings on time levels t_{n+1}, t_n and t_{n-1} are known, the finite difference (3) is well-defined on $\Omega_{t_{n+1}}$. When we introduce the notation $\widehat{\boldsymbol{u}}^i(\boldsymbol{x}^{n+1}) = \boldsymbol{u}^i\big(A_{t_i}\big(A^{-1}_{t_{n+1}}(\boldsymbol{x}_{n+1})\big)\big)$, by substituting (3) into

(1) we get the semidiscrete Navier-Stokes equations for the functions $\boldsymbol{u}^{n+1} : \Omega_{t_{n+1}} \mapsto \mathbb{R}^2$ and $p^{n+1} : \Omega_{t_{n+1}} \mapsto \mathbb{R}$:

$$\frac{3\,\boldsymbol{u}^{n+1}}{2\,\tau} + \Big[(\boldsymbol{u}^{n+1} - \boldsymbol{w}^{n+1}) \cdot \nabla\Big]\boldsymbol{u}^{n+1} + \\ + \nabla p^{n+1} - \nu\,\Delta\boldsymbol{u}^{n+1} = \frac{4\,\widehat{\boldsymbol{u}}^{n} - \widehat{\boldsymbol{u}}^{n-1}}{2\,\tau} \\ \operatorname{div} \boldsymbol{u}^{n+1} = 0\ . \qquad (4)$$

Due to the presence of the convective term $\big[(\boldsymbol{u}^{n+1} - \boldsymbol{w}^{n+1}) \cdot \nabla\big]\boldsymbol{u}^{n+1}$ in the Navier-Stokes equations (4), the system cannot be solved in a straightforward way. Instead, it is first necessary to linearize the equations, i.e. to replace the first occurrence of the sought velocity vector $\boldsymbol{u}^{n+1}$ by some vector $\boldsymbol{u}^{*}$, which is already known. Within this work, Oseen iteration process was used.

The starting point for the finite element discretization of any system of partial differential equations is its weak (variational) formulation. It is obtained by multiplying the classical formulation (4) by an arbitrary test function from the relevant space and integrating over Ω.

To find an approximate solution of the semidiscrete weak Navier-Stokes equations, the finite element method was used. The unstructured, adaptively refined mesh composed of 4000 to 16000 triangular elements. For the velocity and pressure test functions and for the solution, P^{k+1}/P^{k} elements were chosen (P2/P1 and P3/P2 tested). The numerical solution of the discretized problem was implemented using an open-source library Mélina (Martin, 2006), the resulting linear system is solved with the aid of a powerful direct linear solver UMFPACK (Davis, 2006).

For the structural part of the problem, the real, continuously elastic vocal fold was modeled by a rigid body supported by two springs and dampers (similarly as in previous works of Horáček et al (2005)). Such kinematic model reflects two basic modes of the vocal fold motion: vertical shift and rotation. Is is not difficult to derive the equations of motion of the system in the standard form

$$\mathbb{M}\,\ddot{\boldsymbol{q}} + \mathbb{B}\,\dot{\boldsymbol{q}} + \mathbb{K}\,\boldsymbol{q} = \boldsymbol{F}\ , \qquad (5)$$

where $\mathbb{M}$, $\mathbb{B}$, $\mathbb{K}$ are the mass, damping and stiffness matrices, $\boldsymbol{q}$ denotes the vector of generalized coordinates (shift and rotation) and $\boldsymbol{F} = (F_f, M_f)^T$ stands for the vector of generalized forces (vertical force and momentum), induced on the boundary Γ_{VF} by the flow.

The full coupled problem can be solved in the following procedure: Assuming that the solution of the Navier-Stokes equations (1) on a specific time level t and domain Ω_t is known, the total vertical force F_f and momentum M_f, by which the fluid acts on the bottom vocal fold, is given by the integration of the stress vector $\boldsymbol{\tau}$:

$$F_f = \int\limits_{\Gamma^b_{VF}} \tau_2\ d\sigma = \int\limits_{\Gamma^b_{VF}} \sum_{j=1}^{2} \mathbb{T}_{2j}\ n_j\ d\sigma\ , \qquad (6)$$

$$M_f = \int\limits_{\Gamma^b_{VF}} \sum_{l=1}^{2} \Big(\mathbb{T}_{1l}\ n_l\ x_2 - \mathbb{T}_{2l}\ n_l\ x_1\Big) d\sigma \qquad (7)$$

Here $\mathbb{T}$ is the stress tensor and $\boldsymbol{n}$ the unit outer normal to the vocal fold surface. The stress tensor $\mathbb{T}$ is calculated from the pressure and velocity fields $p(t,x)$ and $\boldsymbol{u}(t,x)$ on time level t, according to the constitutive relation valid for Newtonian fluids.

Once the excitation forces are known, we can proceed to the next time level $t+\tau$ by performing one step of the Runge-Kutta method in the time-discretized equations of motion. In this way, we get new system coordinates. These coordinates uniquely determine the shape of the domain $\Omega_{t+\tau}$. With the knowledge of the solution from the previous two time levels, the Navier-Stokes equations can be solved on the new time level $t+\tau$ and new domain $\Omega_{t+\tau}$ using the finite element method.

3. PHYSICAL MODEL

The physical model was proposed as a vocal-fold-shaped element vibrating in the rectangular channel wall. A 4:1 scaled vocal fold model, oscillating only due to coupling with airflow, was designed. In current setup, the upper vocal fold is fixed to avoid difficulties with unsymmetric vocal fold vibration, the bottom one is supported by four flat springs. Best possible effort was made to keep the important dimensionless characteristics (Reynolds and Strouhal numbers) of the model close to the real situation. The shape of the vocal folds was specified according to measurements on excised human larynges, performed in the Institute of Thermomechanics (Šidlof et al, 2004).

The vocal fold model was mounted into a plexiglass wind tunnel. In addition to the PIV system installed to measure the supraglottal flow field, the model was also equipped with accelerometers, pressure transducers and microphones to measure and record vocal fold vibration.

To measure the mean flow in the channel, an ultrasonic flowmeter was mounted near the downstream end of the circular channel. Two accelerometers, fixed under the vibrating vocal fold, were used to record mechanical vibration. The 1:4 scale of the model allowed to use the relatively large, but very sensitive type B&K 4507C without affecting the system significantly.

4. RESULTS

During the numerical simulations, the development of flow and pressure fields for different input flow velocities (or transglottal pressure differences) have been studied. The simulations show the development of the supraglottal jet and evolution of the recirculation vortices within several vocal fold oscillation cycles. The nonstabilized finite element scheme implemented, with a mesh constisting of 16000 triangular P3/P2 elements, allows to reach Reynolds numbers of about 5000, which is sufficient to model the values observed in real human vocal folds.

Figs. 2, 3 demonstrate sample results calculated within a numerical simulation with prescribed parabolic profile of the horizontal velocity component at inlet Γ_{in} (with a maximum of $U_0 = 0.25m/s$). The channel geometry is the same as for the physical model. The mesh was triangular and consisted of 16537 Taylor-Hood (P^3/P^2) elements. The upper vocal fold was fixed, the motion of the bottom one was driven (with no collisions).

The physical model and the measuring equipment mounted provided vibroacoustic data (acceleration signal, dynamic subglottal and supraglottal pressure, acoustic output) and 2D supraglottal flow fields recorded by the PIV.

Fig. 4 shows the measured waveforms and their spectra for a flow rate $Q = 8.58$ l/s, where regular vibrations with impacts occur.

An extensive series of PIV measurements was performed on the vibrating vocal fold model. The flow rate was gradually increased from $Q = 5.33$ l/s (measurement No.001) to $Q = 25.61$ l/s (measurement No.044). Within each of the 44 measurements, approximately 25 PIV records, corresponding to 25 distinct phases of the vocal fold oscillation cycle, were taken. This was realized using the synchronization signal (accelerometer signal converted to TTL) and the time-delay function of the laser control software. Each PIV record consisted of ten PIV measurements of the same phase within ten successive vibration cycles.

Fig. 5 demonstrates the results of one sample measurement (out of 44 in total). This measurement was chosen as a representative case of medium flow rate, large-amplitude regular oscillations, which subjectively correspond the best to normal voice production.

It can be stated that the flow is not perfectly periodical in general. The turbulent structures, developing mainly due to presence of the boundary layer of the jet, interact mutually and with the jet in a disordered, stochastic way; this is why the flow fields of the same phase in successive oscillation cycles are not necessarily identical. The important flow structures, however, are generated periodically in accordance with the frequency of vibration: within each oscillation cycle, a new jet is created with one pair of large vortices propagating along the jet front. The jet attaches to the channel wall and during the closing phase it fades away and eventually disappears, leaving the turbulence to damp out.

5. DISCUSSION

Neither the mathematical nor the physical model was primarily intended for direct comparison with real human vocal folds. The strategy was first to validate the mathematical model using results of the PIV measurements on the physical model; once a satisfactory correspondence between the computational and physical models will be achieved, the geometry and boundary conditions of the mathematical model can be modified in order to reflect the conditions occurring in real vocal folds. For the validation of the model, it was advantageous to use the configuration with one vocal fold moving and the other fixed.

The results from the mathematical and physical model obtained so far seem to correspond when compared visually. It should be noted that there are some aspects, which make a systematic comparison difficult for the time being – the main limitation is the fact that within the mathematical model, the vocal folds are not allowed to collide. The processes accompanying glottal closure are complex and from the algorithmic point of view, the separation of the computational domain into two, necessity to introduce additional boundary conditions and to handle pressure discontinuity when reconnecting the domains represent a very complicated problem. Yet it will be necessary to deal with this task in future, if the mathematical model should be employed to model regular loud phonation.

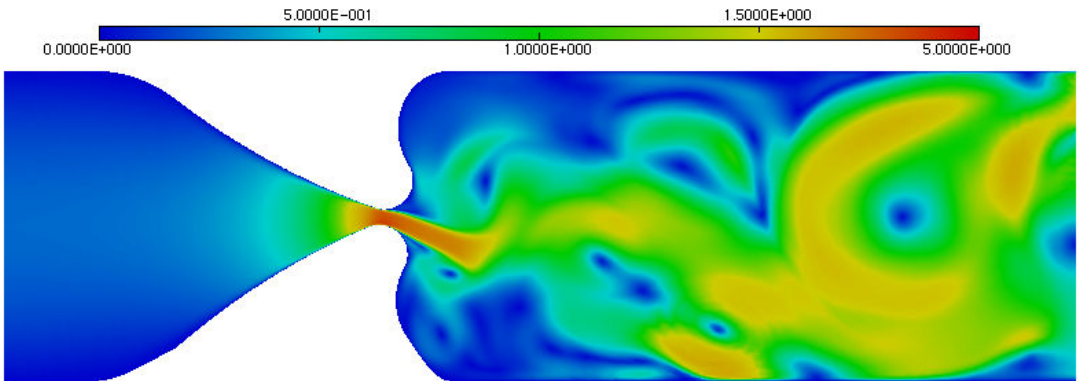

Figure 2: Sample velocity field during the vocal fold vibration cycle – velocity magnitude [m/s].

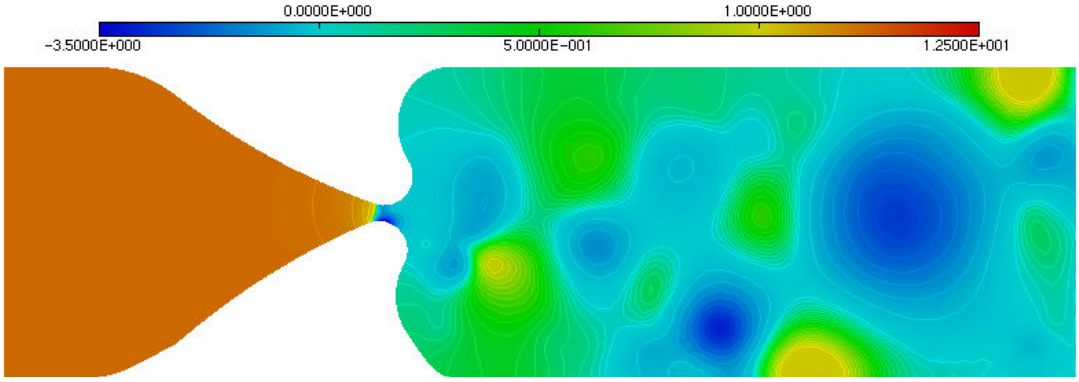

Figure 3: Sample pressure field during the vocal fold vibration cycle - dynamic pressure [Pa].

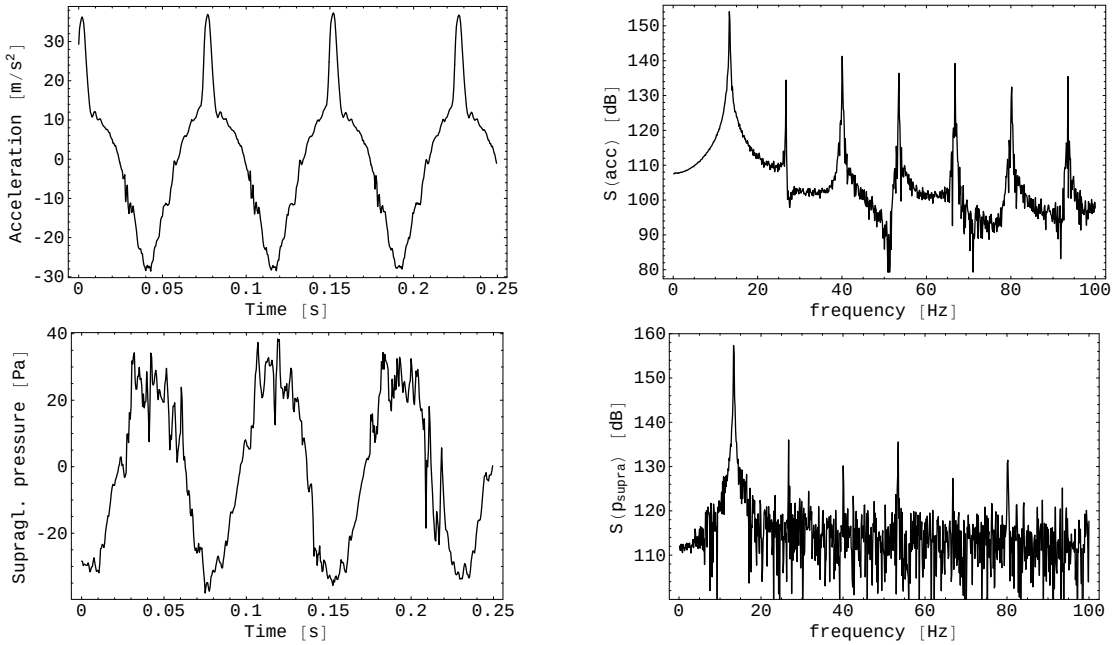

Figure 4: Waveforms and frequency spectra of the acceleration, and supraglottal pressure. Measurement No. 012 – medium flow rate $Q = 8.58$ l/s, ideal for regular vocal fold vibration with an impact in each cycle. Fundamental frequency 13.2 Hz. On the acceleration waveform, the impact is clearly visible as a peak on the positive half-wave.

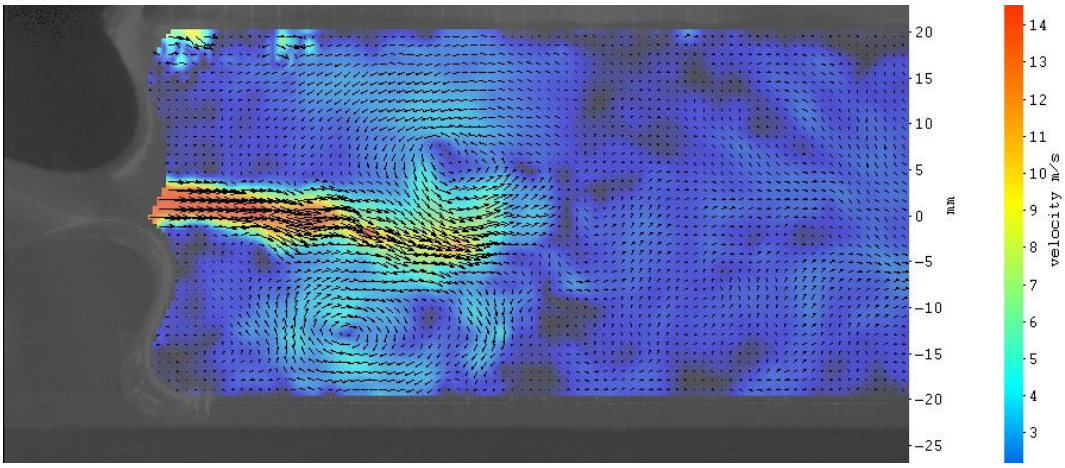

Figure 5: Instantaneous velocity field downstream the glottis. The vocal folds are on the left - the bottom one is fixed, the upper one is moving (the image is reversed vertically with respect to the real setup). The flow direction is from the left to the right. Example taken from measurement No.012. The velocity modulus is in color, arrows show the velocity direction and magnitude. A free jet with a maximum flow velocity of $U \approx 17$ m/s forms between the vocal folds. Two large-scale vortices develop at the sides of the jet front.

6. ACKNOWLEDGMENTS

The research has been financially supported by the Grant Agency of the Academy of Sciences of the Czech Republic, project KJB200760801 *Mathematical modeling and experimental investigation of fluid-structure interaction in human vocal folds*, within the research plan AV0Z20760514. The authors also wish to acknowledge the support of UME ENSTA Paris, who provided all the experimental background.

7. REFERENCES

Davis, T. A., 2006, UMFPack: unsymmetric multifrontal sparse LU factorization package. University of Florida, Gainesville, FL, USA. `http://www.cise.ufl.edu/research/sparse/umfpack/` [Online; accessed 29 November 2006].

Deverge, M., Pelorson, X., Vilain, C., Lagree, P., Chentouf, F., Willems, J., and Hirschberg, A., 2003, Influence of collision on the flow through in-vitro rigid models of the vocal folds. *Journal of the Acoustical Society of America* **114**: 3354–3362.

Erath, B., and Plesniak, M., 2006, The occurrence of the coanda effect in pulsatile flow through static models of the human vocal folds. *Experimental Fluids* **41**: 735–748.

Horáček, J., Šidlof, P., and Švec, J. G., 2005, Numerical simulation of self-oscillations of human vocal folds with Hertz model of impact forces. *Journal of Fluids and Structures* **20**: 853–869.

Kob, M., Krämer, S., Prévot, A., Triep, M., and Brücker, C., 2005, Acoustic measurement of periodic noise generation in a hydrodynamical vocal fold model. In *Proceedings of Forum Acusticum*, Budapest: 2731–2736.

Martin, D., 2006, Finite element library Mélina. Université de Rennes, Unité de Mathématiques Appliquées, ENSTA Paris, France. `http://perso.univ-rennes1.fr/daniel.martin/melina/` [Online; accessed 29 November 2006].

Šidlof, P., Švec, J. G., Horáček, J., Veselý, J., Klepáček, I., and Havlík, R., 2004, Determination of vocal fold geometry from excised human larynges: Methodology and preliminary results. In *International Conference on Voice Physiology and Biomechanics*, Marseille, France.

Thomson, S. L., Mongeau, L., and Frankel, S. H., 2005, Aerodynamic transfer of energy to the vocal folds. *Journal of the Acoustical Society of America 113* **113**: 1689–1700.

Turek, S., 1999, Efficient solvers for incompressible flow problems : An algorithmic and computational approach. Springer-Verlag, Berlin.